*Sensors & Transducers, Vol. 225, Issue 9, September 2018, pp. 8-13*

**Sensors & Transducers**
Published by IFSA Publishing, S. L., 2018
http://www.sensorsportal.com

# An All-dielectric Metasurface Supporting Trapped Mode as a Platform for Sensory Applications

**[1, 2] Anton S. KUPRIIANOV, [1, 3, *] Su XU, [1, 2, *] Wei HAN, [4, 5] Vyacheslav V. KHARDIKOV and [1, 3, 4, *] Vladimir R. TUZ**

[1] International Center of Future Science, Jilin University, 2699 Qianjin Str., Changchun 130012, China
[2] College of Physics, Jilin University, 2699 Qianjin Str., Changchun 130012, China
[3] State Key Laboratory on Integrated Optoelectronics, College of Electronic Science and Engineering, Jilin University, 2699 Qianjin Str., Changchun 130012, China
[4] Institute of Radio Astronomy of NASU, 4, Mystetstv Str., Kharkiv 61002, Ukraine
[5] School of Radio Physics, V. N. Karazin Kharkiv National University, 4, Svobody Sq., Kharkiv 61022, Ukraine
[*] E-mail: xusu@jlu.edu.cn, whan@jlu.edu.cn, tvr@jlu.edu.cn

*Received: 25 June 2018 /Accepted: 31 August 2018 /Published: 30 September 2018*

**Abstract:** The development of the theory of metasurfaces has shown great potential for their use in sensory applications. However, in infrared and visible parts of spectrum the metallic-inclusion-based metasurfaces often face the application obstacles associated with Ohmic losses in metals and fabrication difficulties. Possible solution is to use all-dielectric structures instead of metallic ones. In this study, an all-dielectric resonant metasurface is investigated as a platform for sensory applications in the infrared range. The metasurface is made of an array with unit cell in the form of a single subwavelength dielectric disk having a round eccentric penetrating hole. Resonant states in the transmitted spectra of the metasurface are identified from the comparison with modes inherent in the individual cylindrical dielectric resonators. Correlation between an asymmetry in the geometry of unit cell and formation of the high-quality-factor trapped mode is established. In order to demonstrate the ability of the designed metasurface to serve as a sensor platform, an experimental characterization of the trapped mode is performed in the microwave frequency range.

**Keywords:** Sensor platforms, Photonic structures, Metasurfaces, Metamaterials, Microwave characterization.

## 1. Introduction

Metasurfaces can be potentially used as an ultrathin and flexible platform for sensory applications [1] due to their unique and advantageous ability to support resonances with very narrow bandwidths at any desired frequency based on the structural size of inclusions. Since the metasurfaces operating in the resonant state store electromagnetic energy inside the modes of inclusions, their resonances are highly responsive to the changes in the effective refractive index of the surrounding medium, which provides a basis for sensing operations.

Nevertheless, in the infrared and visible parts of spectrum the implementation of high sensitive sensors based on metasurfaces with metallic inclusions runs into serious obstacles [2-3]. In fact, metallic inclusions in such metasurfaces usually have a very intricate shape, and thus, there is an apparent technological problem with their manufacturing on the nanometer scale. Other severe problem is the absorption, which increases in metallic constituents of metasurfaces with an increase in frequency, and thereby limits their practical applications. Because of losses in metals the corresponding resonances become to be broadened and this degrades the sensitivity of the overall sensory system. Another drawback related to increased absorption is induced thermal effect that can dramatically modify the properties of analytes or even damage them [4].

An alternative way to gain resonant states is to use the dielectric subwavelength particles in metasurface design instead of metallic ones [5]. Each particle behaves as an individual open dielectric resonator exhibiting both electric and magnetic Mie-type resonances [6], which are highly sensitive to the changes of the surrounded conditions. In addition, the particles supporting these resonances can have simple geometrical shapes and therefore can be easily fabricated on nanoscale. These advantages make such all-dielectric metasurfaces feasible to use in the biological and chemical sensors.

On the basis of the Mie-modes theory, several sensors based on all-dielectric metasurfaces have been proposed recently. For instance, an all-dielectric sensing platform based on silicon nanodisks with strong optically-induced magnetic resonances was studied in [7]. It was shown that owning to the strong Mie-type optically-induced magnetic resonances inherent in silicon nanodisks, a dielectric metasurface can serve as a new platform for robust biosensing and detection of biological label-free analytes at their very low concentration in the near-infrared spectral range. Another on-chip biosensing platform based on all-dielectric nanoresonators was reported in [8]. It enables detecting small biomolecules in complex matrices for clinical applications. The operation principle of the system is based on the correlation between the resonant position of the electric dipole mode and the environment conditions.

From a variety of known metasurface designs, we can distinguish a particular class of structures which produce the strongest resonant response due to the excitation of the so-called trapped (dark) modes [9-15]. Such modes appear in metasurfaces provided that their subwavelength particles possess certain structural asymmetry. The degree of the asymmetry determines the strength of electromagnetic coupling between the incident field and the currents induced by this field inside the metasurface particles. Since the electromagnetic field is strongly confined inside the metasurface when the trapped mode is excited, it becomes possible to design highly desirable tunable deep-subwavelength metasurfaces which can serve as a multifunctional platform for light-matter interaction in optical spectroscopic and sensory applications.

In this paper[1] we demonstrate an all-dielectric resonant metasurface with the lattice containing only a single dielectric body per unit cell. Each particle within the lattice behaves as an individual dielectric resonator supporting a set of electric and magnetic modes. We show that the trapped mode with a high quality factor can be excited due to specific asymmetry introduced into the unit cell of the structure. Finally, we discuss the advantages of the proposed metasurface for sensory applications.

## 2. Design and Simulation

In what follows we study an array having a square unit cell ($d_x = d_y = d$), which incorporates a single circular disk with the radius $a_d$ and the height $h_d$ (Fig. 1). Through the disk a round penetrating hole with the radius $a_h$ is made. The hole can be shifted off-center on the distance $\theta$ within the disk along the *y*-axis. When $\theta \neq 0$, the unit cell of the metasurface becomes asymmetric with respect to the *x*-axis, while its symmetry with respect to the *y*-axis remains unchanged. The disks are made from a nonmagnetic dielectric material having the permittivity $\varepsilon_d$. Finally, the lattice is imposed on the top of a thin dielectric substrate (thin compared to the wavelength of incident wave) with the permittivity $\varepsilon_s$ and the thickness $h_s$ to form a complete metasurface.

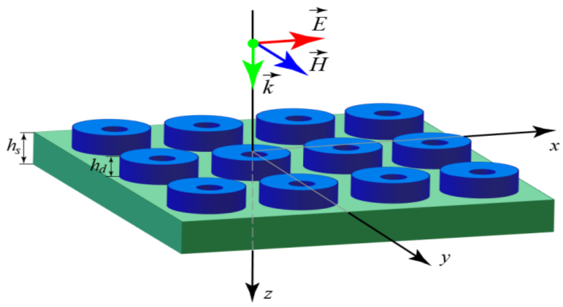


**Fig. 1.** Fragment of an all-dielectric resonant meta-surface whose unit cell consists of a single particle. The particle has the form of a disk with a round penetrating hole made through it. The lattice of disks is placed on a dielectric substrate and the whole structure is under an illumination of a normally incident electromagnetic plane wave whose electric field vector E is oriented along the *x*-axis.

Our main goal is to take advantages of the high quality factor and spectral contrast ratio of the trapped mode resonance for designing a high-performance sensor platform. In order to excite the trapped mode a particular structural asymmetry should be introduced in the unit cell forming a metasurface [9-12]. In the metasurface under study such an asymmetry appears from the eccentric holes, and for the given geometry of the metasurface, the trapped mode can be excited by the normally incident electromagnetic plane wave with nonzero component of the electric field strength **E** along the *x*-axis (Fig. 1).

[1] It is an extended version of Report No. 29 submitted for OPAL' 2018 Conference (Barcelona, Spain) [20].

Following the results of [7], we select the operating wavelength range of $1000 - 2000$ nm with the aim to increase the accuracy of the previously discussed sensor based on the magnetic Mie-type mode. All simulations are made for a metasurface composed of silicon disks ($\varepsilon_d = 13.68$) arranged on a silicon dioxide substrate ($\varepsilon_s = 2.1$). Our numerical simulations of the electromagnetic field scattering by a lattice of volumetric dielectric resonators are based on both original and commercial software.

For comparison purposes, we start our discussion with the demonstration of an electromagnetic response of the metasurface with symmetric unit cell [16-17]. The calculated transmitted spectra $|T|$ for two designs of metasurface having the unit cell in the form of either a solid disk without hole or a disk with centered round penetrating hole are plotted in Fig. 2(a) with solid blue lines and dashed red lines, respectively. In the wavelength range of interest two resonant states having the longest wavelengths are distinguished and marked at the bottom of the figure with blue and red arrows. Note that these resonances are insensitive to the wave polarization (i.e. they appear in the transmitted spectra for both *x*-polarized and *y*-polarized waves).

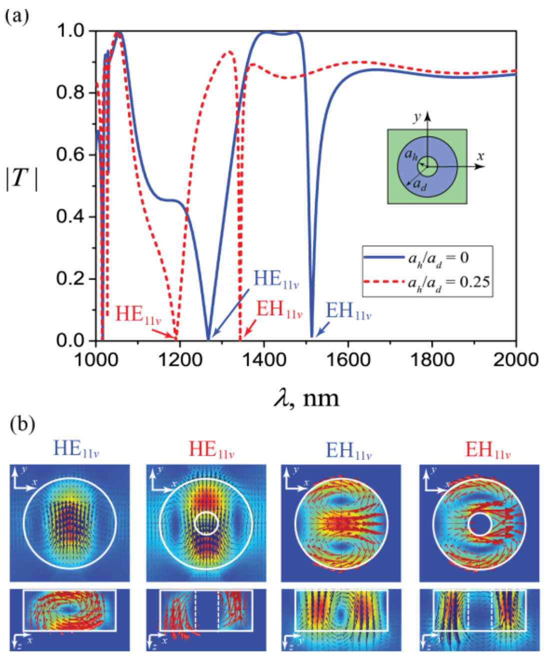


**Fig. 2.** (a) Transmitted spectra of an all-dielectric resonant metasurface possessing a symmetrical unit cell with a solid disk (solid blue line) and a disk having a centered round penetrating hole (dashed red line), and (b) cross-section patterns (total field) of the displacement current (red arrows) and magnetic field (blue arrows) distributions which are calculated within the unit cell at the corresponding resonant wavelengths; $a_d = 310$ nm, $h_d = 200$ nm, $d = 800$ nm, $h_s = 100$ nm.

The cross-section patterns (total field) of the displacement current and magnetic field distributions calculated at the corresponding resonant wavelengths are presented in Fig. 2(b). From these patterns one can conclude that the resonances appear due to existed electromagnetic coupling of the linearly polarized incident wave with the lowest-order (dipole) magnetic mode (first Mie resonance) and electric mode (second Mie resonance) [16] which relate to the hybrid $HE_{11\nu}$-mode and $EH_{11\nu}$-mode of individual cylindrical dielectric resonator, respectively [18-19]. In the notation of hybrid modes the subscripts denote the number of the electromagnetic field variations along the azimuthal, radial and longitudinal directions inside the resonator. The third subscript in the index $p + \nu$ ($p$ = 0,1,...) is introduced to define the number of half-wavelengths standing along the *z*-axis, where $\nu = (2h_d/\lambda_g - p) < 1$, and $\lambda_g$ is the wavelength of corresponding mode of the cylindrical dielectric resonator [19].

The type and characteristics of a hybrid mode can be recognized from its specific resonant pattern associated with the displacement current and magnetic field distributions across the longitudinal and transverse planes of the single resonator located inside the unit cell. In fact, among the parameters of the resonator, the resonant wavelength of the $HE_{11\nu}$-mode is mainly determined by the disk height, whereas that of the $EH_{11\nu}$-mode depends primarily on the disk radius [16]. That is why on the wavelength scale these resonances may have different order depending on the height and radius of the resonator. Along with the lowest-order (dipole) Mie-type modes some higher-order (multipole) modes are also excited by the incident wave in the given metasurface. In the following calculation, multipole modes with shorter wavelengths are excluded from our consideration.

If a round penetrating hole is made in the disk, the resonant states discussed above for a solid disk arise for the modified structure as well [19]. However, since the resonant wavelengths of both Mie-type modes of the individual modified resonator become smaller than those of the original solid disk, the resonant states undergo some blue-shift in the transmitted spectra. This shift stems from the fact that the created hole generally reduces the effective permittivity of the dielectric resonator. It results also in the stronger shift of the resonant wavelength for the $EH_{11\nu}$-mode, since in this case the hole is located exactly in the maximum of its electric field.

The transmitted spectra $|T|$ of a metasurface whose unit cell consists of a single disk having an eccentric round penetrating hole are plotted in Fig. 3(a) for two different displacement distances $\theta$. All resonant states of interest are distinguished as before and are marked in the bottom of the figure with blue and red arrows. One can see that in the transmitted spectra of the modified nonsymmetrical metasurface all previously discussed resonant states related to the lowest-order Mie-type modes generally have almost the same positions as for the metasurface with a symmetric unit cell. Nevertheless, an additional resonance arises in the spectra of the modified structure which is typical for the asymmetric design only. From the analysis of the cross-section patterns (total field) of the displacement current and magnetic field distributions (see Fig. 3(b)) the found resonances are identified as the lowest-order (dipole) magnetic mode, electric mode, and trapped mode, which have an ascending order on the wavelength scale. They are related to the $HE_{11\nu}$-mode, $EH_{11\nu}$-mode, and (transverse electric) $TE_{01\nu}$-mode of the individual cylindrical resonator, respectively. Since the asymmetric unit cell geometry is inherently anisotropic, the trapped mode resonance appears only for the *x*-polarized excitation.

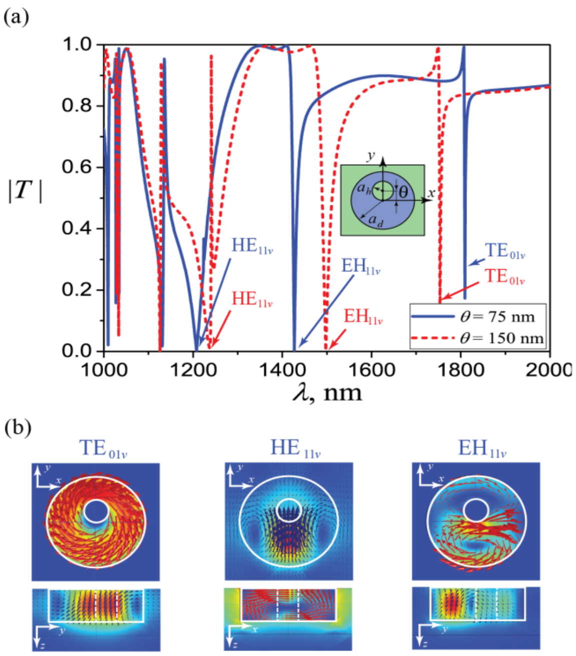


**Fig. 3.** (a) Transmitted spectra of an all-dielectric resonant metasurface possessing an asymmetrical unit cell with a disk having an off-centered round penetrating hole, and (b) cross-section patterns (total field) of the displacement current (red arrows) and magnetic field (blue arrows) distributions which are calculated within the unit cell at the corresponding resonant wavelengths; $a_d = 310$ nm, $h_d = 200$ nm, $d = 800$ nm, $h_s = 100$ nm, and $a_h/a_d = 0.25$.

The trapped mode presented here is a specific resonance intrinsic to structures with an asymmetric design. At the corresponding resonant wavelength, the displacement current of this mode demonstrates a flow with a circular behavior twisting around the center of the unit cell in the plane of the metasurface. Such a current flow produces a magnetic moment oriented along the *z*-axis. Thus, it is directed normally to the metasurface plane. The appearance of such a magnetic moment is an evidence of the artificial magnetism that can be achieved in all-dielectric metasurfaces in the infrared and visible parts of spectrum. Remarkably, the trapped mode appears as an isolated peripheral red-shifted resonance, which, among other thing, is advantageous for use in the sensory applications.

In the case of $TE_{01\nu}$-mode, the presence of the circularly rotated displacement current gives rise to components which oscillate out-of-phase. They are oriented parallel to the *x*-axis and have very low level of electromagnetic coupling to the field of linearly *x*-polarized incident wave. The scattered electromagnetic far field produced by such distribution of the displacement current is very weak. This drastically reduces the coupling between the resonators and free space, and thereby strongly diminishes the radiation losses. The strength of the induced inner field in the trapped mode can reach very high values which ensure a strong resonant response. Similar to characteristics of the dipole Mie- type modes, the spectral line of the trapped mode features a sharp peak-and-trough profile that ensures a high spectral contrast ratio, while the quality factor of such a resonance appears to be much higher than that of the dipole Mie-type modes.

## 3. Experimental Verification

In order to provide an experimental evidence of the trapped mode in all-dielectric metasurfaces, several samples were fabricated for their characterization in the microwave spectral range (1-20 GHz). We have manufactured the metasurfaces by using disks made from a commercially available Taizhou Wangling TP-series ceramic ($\varepsilon_d = 22$, dielectric loss tangent at 10 GHz is $\tan\delta \leq 1\times10^{-3}$) and deposited on the substrate made from a foam ($\varepsilon_s = 1.1$) whose thickness is 45 mm. The samples are manufactured with the use of mechanical cutting and drilling techniques. Each dielectric disk has the radius of 4 mm and thickness of 2.5 mm and is located within a square unit cell of $15\times15$ mm. The radius of penetrating hole is 1 mm. The overall size of the sample is approximately $400\times400$ mm, and it consists of an array of $25\times25$ particles. A fragment of the prepared sample of the all-dielectric metasurface is presented in Fig. 4(a).

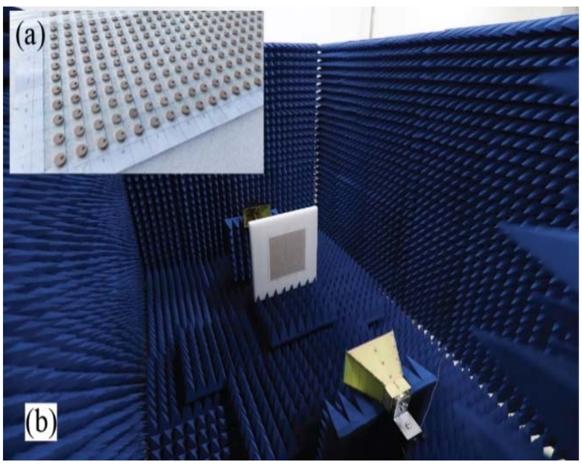


**Fig. 4.** (a) Fragment an all-dielectric resonant metasurface manufactured from ceramic disks using a mechanical cutting technology. The disks are deposited on the foam substrate. All samples are prepared for their characterization in the microwave spectral range $(1-20$ GHz), and (b) the scene of experimental setup with a metasurface under study.

The experimental setup consists of the metasurface under study, which is placed between two wideband double-ridged horn antennas HD-10180DRHA10NK (transmitting and receiving ones) fitted to the Vector Network Analyzer Keysight E5071C. Horn antennas are situated on the axis normal to the plane of the structure. The distance from the transmitting antenna to the sample is selected approximately 1.0 m to ensure a flat front of the irradiating wave. The measurement of transmission spectrum of a metasurface was performed in an anechoic chamber. The scene of an experimental setup with a metasurface under study is given in Fig. 4(b).

Using the Network Analyzer, the $S$-parameters, namely $S_{21}$ – the transmission coefficient ($|S_{21}| = |T|$) of the structure, has been detected and analyzed by the special computer software for two orthogonal polarizations of the incident wave. In order to demonstrate the sensory ability of the proposed design, dry and wet samples were measured. The results of our measurements and corresponding numerical simulations are summarized in Fig. 5.

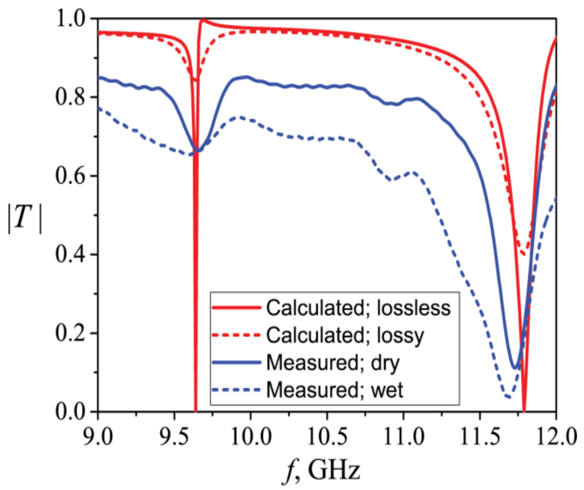


**Fig. 5.** Calculated (red lines) and measured (blue lines) transmitted spectra of the metasurface for the cases of ideal (lossless) and lossy structures; $a_d = 4$ mm, $h_d = 2.5$ mm, $d = 15$ mm, $h_s = 45$ mm, and $a_h/a_d = 0.25$.

Since an asymmetry is introduced into the unit cell of the metasurface with respect to the $x$-axis, an additional resonant peak appears only for the $x$-polarized incident wave near the frequency of 10 GHz. It is an experimental evidence of an excitation of the trapped mode which is supported by our additional numerical simulations for both ideal and lossy structures. We have revealed that the resonance depends critically on the existence of asymmetry inside the unit cell and it persists for the lattices with the unit cells of the other size. One can see that the experimental curves for the dry and wet structures have a significant difference, which confirms the promise of the proposed design for sensory applications.

## 4. Conclusions

In the proposed all-dielectric metasurface, an additional high-quality-factor resonant state appears if certain structure asymmetry is created. It is referred to the trapped mode whose electromagnetic field is strongly confined inside the structure, while being weakly coupled to free space.

Similar to characteristics of the dipole modes, the spectral line of the trapped mode acquires a sharp peak-and-trough profile, whereas the quality factor of such resonance can be much higher than that of the Mie-type modes. Moreover, the quality factor of such trapped mode is fully controlled by the degree of structural asymmetry. The distinctive feature of the trapped mode is that it is an alone-standing lowest-frequency resonance (i.e. in term of wavelength it acquires a giant red-shift), and, thus, this resonance can be easily recognized and controlled among other resonances in the spectrum.

In summary, we have made a proof of concept of the proposed all-dielectric metasurface with samples fabricated from inexpensive materials and production technologies, which yields particles manufactured from the commercially available ceramic for metasurface characterization in the microwave range. The results obtained here allow us to conclude that the proposed metasurface has a potential to serve as a new platform for sensory applications in the infrared spectral range.

## Acknowledgements

Authors acknowledge OPAL' 2018 Conference Organizing Committee and its Chairman prof. Sergey Y. Yurish for their invitation to submit an extended version of our conference Report to this special issue of Sensors & Transducers journal.

## References

[1]. C. L. Holloway, E. F. Kuester, J. A. Gordon, J. O'Hara, J. Booth, D. R. Smith, An overview of the theory and applications of metasurfaces: The two-dimensional equivalents of metamaterials, *IEEE Antennas Propag. Mag.*, Vol. 54, Issue 2, 2012, pp. 10-35.

[2]. R. Singh, W. Cao, I. Al-Naib, L. Cong, W. Withayachumnankul, W. Zhang, Ultrasensitive terahertz sensing with high-Q Fano resonances in metasurfaces, *Appl. Phys. Lett.*, Vol. 105, Issue 17, 2014, pp. 171101.

[3]. L. Cong, S. Tan, R. Yahiaoui, F. Yan, W. Zhang, R. Singh, Experimental demonstration of ultrasensitive sensing with terahertz metamaterial absorbers: A comparison with the metasurfaces, *Appl. Phys. Lett.*, Vol. 106, Issue 3, 2015, pp. 031107.

[4]. Y. Ueba1, J. Takahara, Spectral control of thermal radiation by metasurface with split-ring resonator, *Appl. Phys. Express*, Vol. 5, Issue 12, 2012, pp. 122001-1 – 122001-3.

[5]. A. Krasnok, M. Caldarola, N. Bonod, A. Alu, Spectroscopy and biosensing with optically resonant dielectric nanostructures, *Adv. Optical Mater.*, Vol. 6, Issue 5, 2018, pp. 1701094.

[6]. S. Kruk, Yu. S. Kivshar, Functional meta-optics and nanophotonics govern by Mie resonances, *ACS Photonics*, Vol. 4, Issue 11, 2017, pp. 2638-2649.

[7]. N. Bontempi, K. E. Chong, H. W. Orton, I. Staude, D.-Y. Choi, I. Alessandri, Y. S. Kivshar, D. N. Neshev, Highly sensitive biosensors based on all-dielectric nanoresonators, *Nanoscale*, Vol. 9, Issue 15, 2017, pp. 4972-4980.

[8]. O. Yavas, M. Svedendahl, P. Dobosz, V. Sanz, R. Quidant, On-a-chip biosensing based on all-dielectric nanoresonators, *Nano Lett.*, Vol. 17, Issue 7, 2017, pp. 4421-4426.

[9]. S. Prosvirnin, S. Zouhdi, Resonances of closed modes in thin arrays of complex particles, in Advances in Electromagnetics of Complex Media and Metamaterials, S. Zouhdi and M. Arsalane, Eds., *The Netherlands: Springer, Dordrecht: Kluwer Academic Publishers*, 2003, pp. 281-290.

[10]. V. Fedotov, M. Rose, S. L. Prosvirnin, N. Papasimakis, N. I. Zheludev, Sharp trapped-mode resonances in planar metamaterials with a broken structural symmetry, *Phys. Rev. Lett.*, Vol. 99, Issue 14, 2007, pp. 147401.

[11]. V. Khardikov, E. Iarko, S. Prosvirnin, Trapping of light by metal arrays, *J. Opt.*, Vol. 12, Issue 4, 2010, pp. 045102.

[12]. V. R. Tuz, V. V. Khardikov, A. S. Kupriianov, K. L. Domina, S. Xu, H. Wang, H.-B. Sun, High-quality trapped modes in all-dielectric metamaterials, *Opt. Express*, Vol. 26, Issue 3, 2018, pp. 2905-2916.

[13]. V. R. Tuz, S. L. Prosvirnin, L. A. Kochetova, Optical bistability involving planar metamaterials with broken structural symmetry, *Phys. Rev. B*, Vol. 82, Issue 23, 2010, pp. 233402.

[14]. V. R. Tuz, S. L. Prosvirnin, All-optical switching in metamaterial with high structural symmetry, *Eur. Phys. J.: Appl. Phys.*, Vol. 56, Issue 3, 2011, pp. 30401.

[15]. V. Khardikov, P. Mladyonov, S. Prosvirnin, V. Tuz, Electromagnetic wave diffraction by periodic planar metamaterials with nonlinear constituents, in Contemporary Optoelectronics: Materials, Metamaterials and Device Applications, O. Shulika and I. Sukhoivanov, Eds., Dordrecht, *The Netherlands: Springer*, Vol. 199, 2016, pp. 81-98.

[16]. M. Decker, I. Staude, M. Falkner, J. Dominguez, D. N. Neshev, I. Brener, T. Pertsch, Yu. S. Kivshar, High efficiency dielectric Huygens' surfaces, *Adv. Opt. Mater.*, Vol. 3, Issue 6, 2015, pp. 813-820.

[17]. X. Liu, K. Fan, I. V. Shadrivov, W. J. Padilla, Experimental realization of a terahertz all-dielectric metasurface absorber, *Opt. Express*, Vol. 25, Issue 1, 2017, pp. 191-201.

[18]. D. R. Abujetas, R. Paniagua-Dominguez, J. A. Sanchez-Gil, Unraveling the Janus role of Mie resonances and leaky/guided modes in semiconductor nanowire absorption for enhanced light harvesting, *ACS Photonics*, Vol. 2, Issue 7, 2015, pp. 921-929.

[19]. R. K. Mongia, P. Bhartia, Dielectric resonator antennas – A review and general design relations for resonant frequency and bandwidth, *Int. J. RF Microw. Comput. Aided Eng.*, Vol. 4, Issue 3, 1994, pp. 230-247.

[20]. S. Xu, V. Khardikov, V. Tuz, Trapped modes in a single-particle all-dielectric planar metamaterial, in *Proceedings of the 1st International Conference on Optics, Photonics and Lasers (OPAL-2018)*, Barcelona, Spain, 9-11 May, 2018, pp. 70-73.